



# Article

# Parameter Extraction of Three Diode Solar Photovoltaic Model Using Improved Grey Wolf Optimizer

Abd-ElHady Ramadan <sup>1</sup>, Salah Kamel <sup>1</sup> , Tahir Khurshaid <sup>2,\*</sup> , Seung-Ryle Oh <sup>3</sup> and Sang-Bong Rhee <sup>2,\*</sup>

<sup>1</sup> Department of Electrical Engineering, Faculty of Engineering, Aswan University, Aswan 81542, Egypt; eng.abdalahady@gmail.com (A.-E.R.); skamel@aswu.edu.eg (S.K.)

<sup>2</sup> Department of Electrical Engineering, Yeungnam University, Gyeongsan 38541, Korea

<sup>3</sup> Korea Electric Power Company (KEPCO), Deajon 24056, Korea; exp0510@kepco.co.kr

\* Correspondence: Authors: tahir@ynu.ac.kr (T.K.); rrsd@yu.ac.kr (S.-B.R.)

**Abstract:** The enhancement of photovoltaic (PV) energy systems relies on an accurate PV model. Researchers have made significant efforts to extract PV parameters due to their nonlinear characteristics of the PV system, and the lack of information from the manufacturers' PV system datasheet. PV parameters estimation using optimization algorithms is a challenging problem in which a wide range of research has been conducted. The idea behind this challenge is the selection of a proper PV model and algorithm to estimate the accurate parameters of this model. In this paper, a new application of the improved gray wolf optimizer (I-GWO) is proposed to estimate the parameters' values that achieve an accurate PV three diode model (TDM) in a perfect and robust manner. The PV TDM is developed to represent the effect of grain boundaries and large leakage current in the PV system. I-GWO is developed with the aim of improving population, exploration and exploitation balance and convergence of the original GWO. The performance of I-GWO is compared with other well-known optimization algorithms. I-GWO is evaluated through two different applications. In the first application, the real data from RTC furnace is applied and in the second one, the real data of PTW polycrystalline PV panel is applied. The results are compared with different evaluation factors (root mean square error (RMSE), current absolute error and statistical analysis for multiple independent runs). I-GWO achieved the lowest RMSE values in comparison with other algorithms. The RMSE values for the two applications are 0.00098331 and 0.0024276, respectively. Based on quantitative and qualitative performance evaluation, it can be concluded that the estimated parameters of TDM by I-GWO are more accurate than those obtained by other studied optimization algorithms.

**Keywords:** solar photovoltaic; three diode model; parameters; optimization; improved gray wolf optimizer; RMSE; polycrystalline; statistical analysis



**Citation:** Ramadan, A.-E.; Kamel, S.; Khurshaid, T.; Oh, S.-R.; Rhee, S.-B. Parameter Extraction of Three Diode Solar Photovoltaic Model Using Improved Grey Wolf Optimizer. *Sustainability* **2021**, *13*, 6963. <https://doi.org/10.3390/su13126963>

Academic Editors:  
Francesco Riganti-Fulginei and  
Simone Quondam-Antonio

Received: 22 April 2021

Accepted: 16 June 2021

Published: 21 June 2021

**Publisher's Note:** MDPI stays neutral with regard to jurisdictional claims in published maps and institutional affiliations.



**Copyright:** © 2021 by the authors. Licensee MDPI, Basel, Switzerland. This article is an open access article distributed under the terms and conditions of the Creative Commons Attribution (CC BY) license (<https://creativecommons.org/licenses/by/4.0/>).

## 1. Introduction

Solar energy plays a large role in saving the environment, helping people socially and economically, and creating jobs and research. Solar energy has many advantages and it is a clean energy source that has many different uses [1–3]. In contrast, fossil fuel resources are decreased and have a negative environmental impact; hence, solar energy is considered one of the most promising alternative energy sources [4,5].

Nowadays, solar energy has many applications. One of these applications is installing solar cells in residential units and connecting them to the main electrical network. Connecting residential solar energy systems to the main network requires an accurate model to analyze and describe the voltage and current changes to these systems [6]. There are also many other applications of solar energy, which also require for its development to an accurate mathematical model for the solar system, such as solar water heating, solar heating of buildings, solar-distillation, solar-pumping, solar drying of agricultural and animal products, and solar furnaces [7–9].

One of the biggest challenges limiting the usage of solar energy is the huge cost of manufacturing and installation. PV cell has nonlinear current-voltage characteristics and nonlinear power-voltage characteristics. Due to these nonlinear properties, the actual operation of the solar cells varies with different operating conditions such as irradiance/temperature conditions, which change over the day and over the seasons. These changes make it difficult to get the best efficiency of the solar cell by relying on the operating conditions of the factory [10].

Modeling of PV systems is considered one of the important stages in the design and manufacturing of PV systems, because of the important information collected from the PV model that helps to predict the PV characteristics under different operating conditions, and thus increase the operating efficiency of these cells [11].

Different models have been proposed in the literature for the PV systems. Single diode model (SDM) and double diode model (DDM) are considered the most popular models in literature. PV cell is a semiconductor PN junction that converts sunlight to an electrical current. The ideal model of the solar cell can be represented by an ideal current source, but the real model of a solar cell should take into consideration the losses in light and current that can be represented electrically by diodes. The model that has a greater number of diodes represents more losses. SDM has one diode that represents the loss in the quasi-neutral zone. A SDM has five estimated parameters [11–14]. DDM is developed to represent the loss in recombination at lower irradiance by adding a second diode to the model. The total estimated parameters in DDM are seven parameters [15–17].

The triple diode model (TDM) is developed to represent the leakage in grain boundaries in PV system by adding a third diode to the model. The total estimated parameters in TDM are nine parameters [18–26]. Although the accuracy of the model increased by increasing the number of diodes, the complexity of the model also increased.

The challenge of parameters estimation of these models using optimization algorithms has been discussed in many previous works. A review about the application of evolutionary algorithms (EA) on PV parameters estimation has been presented in a previous study [27]. Different types of evolutionary algorithms (EA) have been discussed in [27], such as EA based on swarm intelligence, EA based on physical theory and EA based on hybridization between different types. They concluded that hybridized techniques have a better accuracy for PV parameters estimation, but with less convergence speed. A new method that combines harrier hawk optimization (HHO) with computation method to extract the parameters of the PV TDM has been presented in [28]. Four parameters are extracted by equations and the other five parameters are estimated through HHO. An improved equilibrium optimizer was presented in [29], to estimate the PV parameters of SDM and DDM. The enhancement is achieved using linear reduction diversity technique to improve the diversity of the population until getting the best estimated model parameters that achieve the least RMSE between real measure data and the model which is considered as the best solution. Another improvement for moth-flame optimizer was presented in [30], to estimate the PV parameters of SDM and DDM. The improvement is based on double flame generation. Grasshopper Optimization Algorithm was presented to estimate the PV parameters of TDM in [31]. An intelligent grey wolf optimizer was presented in [32], to estimate the PV panel parameters of SDM and DDM. The idea behind intelligent gray wolf optimizer is the incorporation of opposition based learning to the conventional gray wolf optimizer (GWO) to enhance the exploration and exploitation phases.

This paper is considered a completion in this track, but here the study considers an application of another improvement for GWO which was presented in [33] and discusses the effect of this improvement on PV parameters estimation of TDM. The improved GWO algorithm is called I-GWO. I-GWO is developed with the aim of improving population, exploration and exploitation balance and convergence of the original GWO. The I-GWO is applied to estimate the parameters of TDM for 57 mm diameter commercial silicon R.T.C France solar cell (1000 W/m<sup>2</sup> at 33 °C). For more comprehensive results, the I-GWO is applied to estimate the parameters of TDM for Photowatt-PWP201 PV module.

This module contains 36 polycrystalline silicon cells connected in series and operating at an irradiance of 1000 W/m<sup>2</sup> and temperature of 45 °C. The obtained results in the two applications from I-GWO are compared with the original GWO and other recent optimization algorithms. The obtained results in the two applications are evaluated using different evaluation methods. The accuracy of the studied algorithms are evaluated using root mean square error (RMSE) and absolute error between the real output current and the estimated current by TDM. The speed of the algorithms is compared through the convergence curves. The robustness of the algorithms is compared through the statistical analysis for different independent runs. Minimum, maximum, average and standard deviation statistical values are calculated for all runs. The behaviors of the current-voltage characteristics and power-voltage characteristics at different operating temperatures are discussed for the optimized TDM in the two applications.

## 2. Mathematical Mode and Optimization Problem

This section discusses the main components of TDM and PV panel as well as the main objective functions of the studied optimization problem.

### 2.1. Model of TDM and PV Panel

The TDM consists of an ideal current source to represent the ideal solar cell, three diodes to represent different current losses, series and shunt resistance [34,35]. The TDM equivalent circuit is shown in Figure 1. Each component is discussed as:

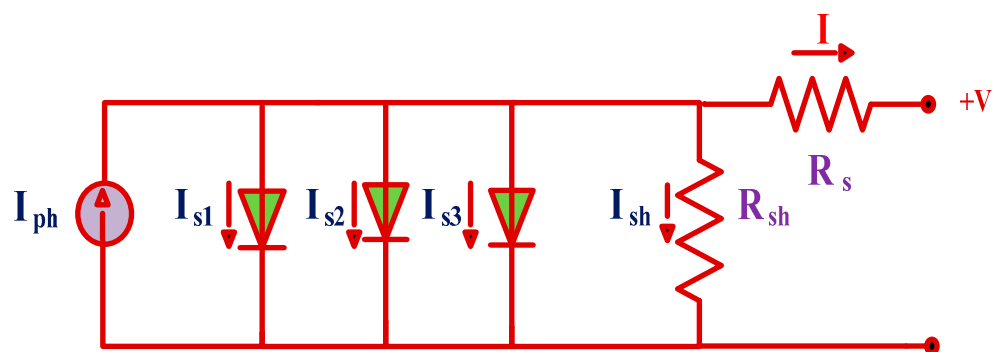


Figure 1. PV TDM.

Current source represents the photo-generated current ( $I_{ph}$ ).

- First diode represents the effect of diffusion current ( $I_{s1}$ ).
- First diode represents the effect of diffusion current ( $I_{s1}$ ).
- Second diode represents the effect of recombination current ( $I_{s2}$ ).
- Third diode represents the effect of grain boundaries and large leakage current ( $I_{s3}$ ).
- Series resistance represents the semiconductor material resistance at neutral regions ( $R_s$ ).
- Shunt resistance represents the current leakage resistance across the P-N junction of PV system ( $R_{sh}$ ).

Equations (1) and (2) describe the total output current ( $I$ ) of the mathematical model of TDM.

$$I = I_{ph} - I_{s1} - I_{s2} - I_{s3} - I_{sh} \quad (1)$$

$$I = I_{ph} - I_{s1} \left[ \exp\left(\frac{q(V+R_s I)}{\eta_1 K T}\right) - 1 \right] - I_{s2} \left[ \exp\left(\frac{q(V+R_s I)}{\eta_2 K T}\right) - 1 \right] - I_{s3} \left[ \exp\left(\frac{q(V+R_s I)}{\eta_3 K T}\right) - 1 \right] - \frac{(V+R_s I)}{R_{sh}} \quad (2)$$

A combination between series solar cells represents a PV module and a combination between parallel modules represents a PV array as shown in Figure 2. The total output current ( $I$ ) of the mathematical model of TDM for PV module is described by Equation (3).

$$\begin{aligned} I/N_p = I_{ph} - I_{s1} \left[ \exp\left(\frac{q(V/N_s + R_s I/N_p)}{\eta_1 K T}\right) - 1 \right] - I_{s2} \left[ \exp\left(\frac{q(V/N_s + R_s I/N_p)}{\eta_2 K T}\right) - 1 \right] - \\ I_{s3} \left[ \exp\left(\frac{q(V/N_s + R_s I/N_p)}{\eta_3 K T}\right) - 1 \right] - \frac{(V/N_s + R_s I/N_p)}{R_{sh}} \end{aligned} \quad (3)$$

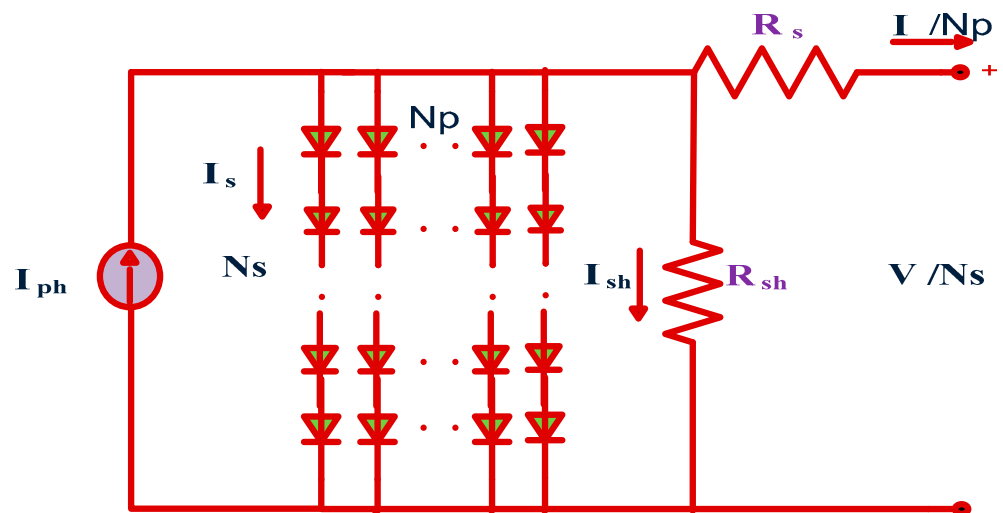


Figure 2. PV module.

## 2.2. Objective Function

In TDM, nine estimated parameters are considered  $[R_s, R_{sh}, I_{ph}, I_{s1}, I_{s2}, I_{s3}, \eta_1, \eta_2, \eta_3]$  and they can be represented in one vector  $x = [x_1, x_2, x_3, x_4, x_5, x_6, x_7, x_8, x_9]$ . The optimization problem in this work is to estimate the best values of TDM parameters to reduce the error between experimental and estimated output current; hence the objective function of the current optimization problem is described by Equation (4). The best estimated parameters are those that achieve the lowest RMSE for the objective function, as shown by Equation (5) [36,37]. The objective function of the TDM for PV module is described by Equation (6) [10]. The main steps of the optimization process are summarized in Figure 3.

$$\begin{aligned} f_{TDM}(V, I, X) = I - X_3 + X_4 \left[ \exp\left(\frac{q(V + R_s I)}{X_7 K T}\right) - 1 \right] + X_5 \left[ \exp\left(\frac{q(V + R_s I)}{X_8 K T}\right) - 1 \right] + \\ X_6 \left[ \exp\left(\frac{q(V + R_s I)}{X_9 K T}\right) - 1 \right] + \frac{(V + X_1 I)}{X_2} \end{aligned} \quad (4)$$

$$RMSE = \sqrt{\frac{1}{N} \sum_{k=1}^N f^2(V_{tm}, I_{tm}, X)} \quad (5)$$

where,  $V_{tm}$  and  $I_{tm}$  are the measured voltage and current,  $X$  is the estimated parameters,  $N$  is the maximum number of the measured data.

$$\begin{aligned} f_{TDM}(V, I, X) = I - X_3 + X_4 \left[ \exp\left(\frac{q(V/N_s + R_s I/N_p)}{X_7 K T}\right) - 1 \right] + X_5 \left[ \exp\left(\frac{q(V/N_s + R_s I/N_p)}{X_8 K T}\right) - 1 \right] + \\ X_6 \left[ \exp\left(\frac{q(V/N_s + R_s I/N_p)}{X_9 K T}\right) - 1 \right] + \frac{(V/N_s + X_1 I/N_p)}{X_2} \end{aligned} \quad (6)$$

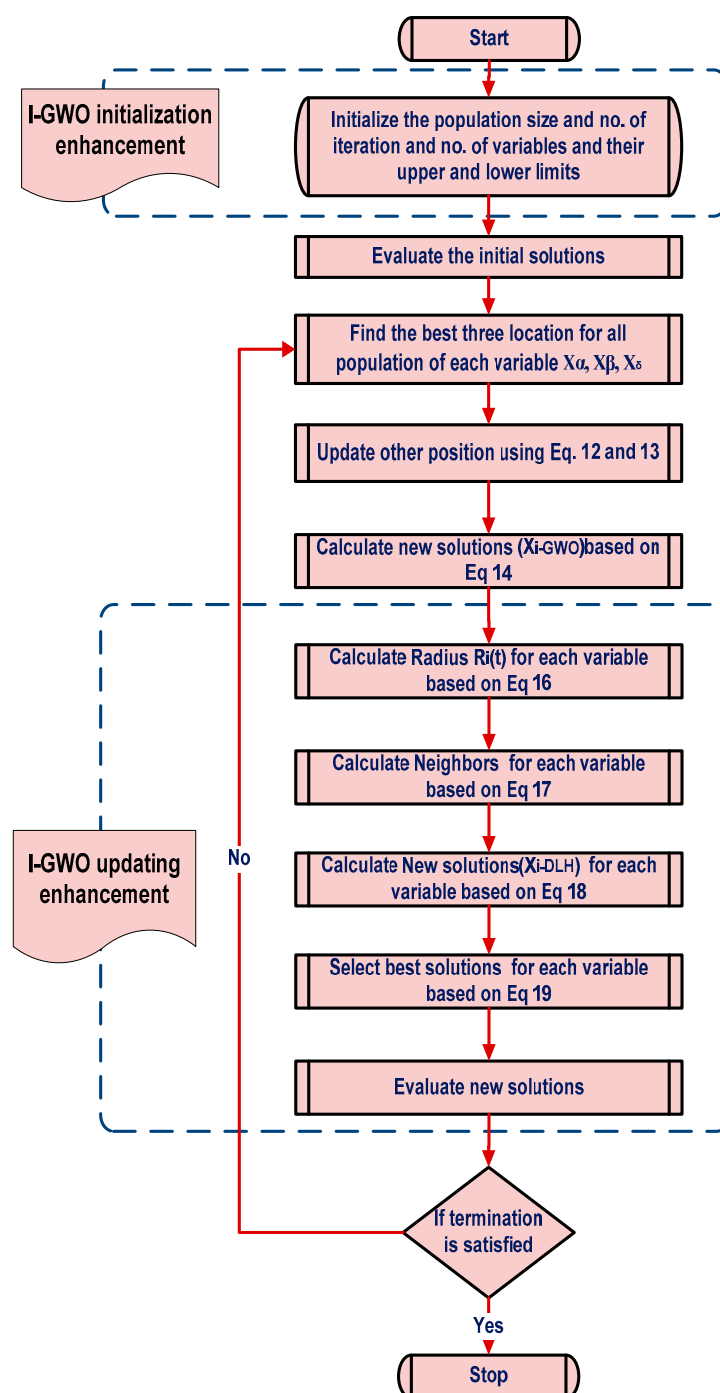


Figure 3. I-GWO flowchart.

### 3. Grey Wolf Optimizers

In this section, both original GWO and I-GWO are discussed.

#### 3.1. Grey Wolf Optimizer (GWO)

GWO is inspired by the grey wolf's manner in attacking their prey [38–42]. GWO determines the way to the best solution based on the first three best solutions inspired from three wolf leaders. The main steps of GWO are described as follows:

The wolf  $X_P(t)$  detects the prey position  $X_P(t)$  to surround it, as shown by Equation (7).

$$D = |C \times X_P(t) - X(t)| \quad (7)$$

Movement towards the prey Equation (8).

$$X(t+1) = X_P(t) - A \times D \quad (8)$$

where,  $A$  and  $C$  are given by Equations (9) and (10), respectively.

$$A = 2 \times A - r_1 - a(t) \quad (9)$$

$$C = 2 \times r_2 \quad (10)$$

where,  $a(t)$  is a factor decreased depending on the maximum number of iterations as described in (11).

$$a(t) = 2 - (2 \times t) / \text{MaxIter} \quad (11)$$

Tracking the prey considering the best three positions for the three wolf leaders  $\alpha$ ,  $\beta$  and  $\delta$ , with positions  $X_\alpha$ ,  $X_\beta$  and  $X_\delta$ . Each wolf updates its position depending on the three best leaders, as given in Equation (12).

$$\begin{aligned} X_{i1}(t) &= X_\alpha(t) - A_{i1} \times D_\alpha(t) \\ X_{i2}(t) &= X_\beta(t) - A_{i2} \times D_\beta(t) \\ X_{i3}(t) &= X_\delta(t) - A_{i3} \times D_\delta(t) \end{aligned} \quad (12)$$

where,  $D_\alpha$ ,  $D_\beta$  and  $D_\delta$  are calculated from Equation (13).

$$\begin{aligned} D_\alpha &= |C_1 \times X_\alpha - X_i| \\ D_\beta &= |C_2 \times X_\beta - X_i| \\ D_\delta &= |C_3 \times X_\delta - X_i| \end{aligned} \quad (13)$$

The final best position is updated depending on the three best leaders' positions as given in Equation (14).

$$X(t+1) = \frac{X_{i1}(t) + X_{i2}(t) + X_{i3}(t)}{3} \quad (14)$$

### 3.2. Improved Grey Wolf Optimizer (I-GWO)

I-GWO was developed to improve the performance of the original GWO by reducing the probability of fall in local optima [33]. The improvement is achieved by a new search strategy that includes selecting and updating steps highlighted by a dashed line in flowchart.

The detailed description of the enhancement is as follows:

- Increasing the initialization by random distribution for  $N$  wolves within the search range as described in Equation (15).

$$X_{ij} = LB_j + \text{rand}_j[0,1](UB_j - LB_j) \quad (15)$$

where,  $i \in [1, N]$  problem dimension,  $j \in [1, D]$  problem dimension.  $LB$  and  $UB$  are the search low and upper limits, respectively.

- The tracking behavior is enhanced using dimension learning-based hunting technique (DLH). In DLH, each wolf learns from its neighbors. The construction of the neighbors according to the calculated radius are calculated by Equations (16) and (17). The new positions are determined using Equation (18).

The best position is determined by Equation (19) considering  $X_{i\text{-GWO}}(t+1)$  that determined is by Equation (15).

$$R_i(t) = \|X_i(t) - X_{i\text{-GWO}}(t+1)\| \quad (16)$$

$$N_i(t) = \{X_j(t) \mid D_i(X_i(t), X_j(t)) \leq R_i(t), X_j(t) \in Pop\} \quad (17)$$

$$X_{i=DLH,d}(t+1) = X_{i,d}(t) + rand \times (X_{n,d}(d) - X_{r,d}(t)) \quad (18)$$

$$X_i(t+1) = \begin{cases} X_{i-GWO}(t+1) & \text{if } f(X_{i-GWO}) < f(X_{i=DLH}) \\ X_{i=DLH}(t+1) & \text{otherwise} \end{cases} \quad (19)$$

The flowchart of I-GWO is shown in Figure 3.

The main steps of I-GWO can be described as follows:

(Initialization steps)

- Random distribution for N wolfs within the search range, as shown by (15)
- (Main steps)
- For iteration = 1 to maximum iteration
- Find three wolf leaders  $\alpha$ ,  $\beta$  and  $\delta$ ,
- Update three wolf leaders' positions  $X_\alpha$ ,  $X_\beta$  and  $X_\delta$  using (12) and (13).
- Calculate the best position  $X_{i-GWO}$  using (14)
- (Updating improvement steps (DLH))
- Calculate radius to construction of the neighbors using (16)
- Determine the neighbors using Equation (17)
- Calculate new solution  $X_{i=DLH,d}(t+1)$  using (18)
- Select the best position between  $X_{i=DLH,d}(t+1)$  and  $X_{i-GWO}(t+1)$  using (19)
- End for loop

#### 4. Results

This section discusses the performance of I-GWO when it is applied to estimate the parameters of TDM for different real PV systems. Different evaluation methods are used for results, evaluation and analysis. Two different applications, the real data from RTC furnace and the real data of PTW polycrystalline PV panel, are considered in the analysis.

##### 4.1. Application #1:

In this application, the real data of 57 mm diameter commercial silicon R.T.C France solar cell (under 1000 W/m<sup>2</sup> at 33 °C) are used for parameters estimation of the TDM [43]. A comparison between the obtained root mean square error (RMSE) values of I-GWO and other recent optimization algorithms is presented in Table 1. The parameters of each algorithm are listed in Table 2. The convergence curve of all algorithms is shown in Figure 4. The I-GWO has a RMSE value better than the original GWO as well as other compared algorithms. Moreover, I-GWO has an accepted convergence speed as shown in Figure 4. The stability of I-GWO is tested from the statistical analysis of 30 independent runs as observed in Table 3 and the boxplot in Figure 5. A graphical display of the absolute error between the real measured output current values and the model output value in Equation (20) is shown in Figures 6–8 to depict the characteristic curves of the current-voltage and the power curve for the real PV measured data and the calculated by different algorithms. The characteristic curve of the current-voltage and the power curve for the TDM estimated by I-GWO at different temperatures is displayed in Figures 9 and 10, respectively.

$$\text{Current Absolut error} = \sqrt[2]{(I - I_{\text{estimated}})^2} \quad (20)$$

##### 4.2. Application #2:

In this application, the real data of Photowatt-PWP201 PV module are used [44–46]. This module contains 36 polycrystalline silicon cells connected in series and operating at an irradiance of 1000 W/m<sup>2</sup> and temperature of 45 °C. A comparison between the obtained root mean square error (RMSE) value of I-GWO and other recent optimization algorithms is presented in Table 4. The convergence curves of all algorithms are shown in Figure 11. The I-GWO has a RMSE value better than the original GWO, as well as other compared algorithms, except it is slightly better than HBO. The stability of I-GWO



is tested from the statistical analysis of 30 independent runs as shown in Table 5 and the boxplot in Figure 12. A graphical display of the absolute error between the real measured output current values and the model output value is shown in Figures 13–15 show the characteristic curves of the current-voltage and the power curve for the real PV measured data and the calculated by different algorithms. The characteristic curves of the current-voltage and the power curves for the TDM estimated by I-GWO at different temperatures are shown in Figures 16 and 17, respectively.

**Table 1.** Estimated parameters and RMSE for I-GWO and other optimization algorithms.

	IGWO	GWO	HBO	MRFO	HHO
$R_s(\Omega)$	0.0367	0.043821	0.040	0.03634	0.018333
$R_{sh}(\Omega)$	54.888	59.64	59.997	53.9246	92.25011
$I_{ph}(A)$	0.7607	0.7619	0.7608	0.76078	0.764769
$I_{sd1}(A)$	$2.27 \times 10^{-7}$	$1.38 \times 10^{-10}$	$6.97 \times 10^{-7}$	$2.67 \times 10^{-8}$	$3.82 \times 10^{-6}$
$I_{sd2}(A)$	$3.14 \times 10^{-7}$	$2.51 \times 10^{-10}$	$1.00 \times 10^{-10}$	$1.54 \times 10^{-8}$	$2.71 \times 10^{-6}$
$I_{sd3}(A)$	$2.34 \times 10^{-7}$	$4.07 \times 10^{-6}$	1.59472	$3.17 \times 10^{-7}$	$1.28 \times 10^{-6}$
N1	1.9256	1.6677	1.009	1.9076	1.882327
N2	1.9600	1.0181	1.0082	1.8674	1.891646
N3	1.4500	1.9182	1.3083	1.475	1.891677
RMSE	0.00098331	0.00191	0.001120	0.000986002	0.007721

**Table 2.** Parameters setting for each studied algorithm.

Algorithm	Parameter Setting	
I-GWO	$r1 = \text{rand}()$	$r2 = \text{rand}()$
GWO	$r1 = \text{rand}()$	$r2 = \text{rand}()$
HBO	degree = 3	
MRFO	NP = 1000	S = 2

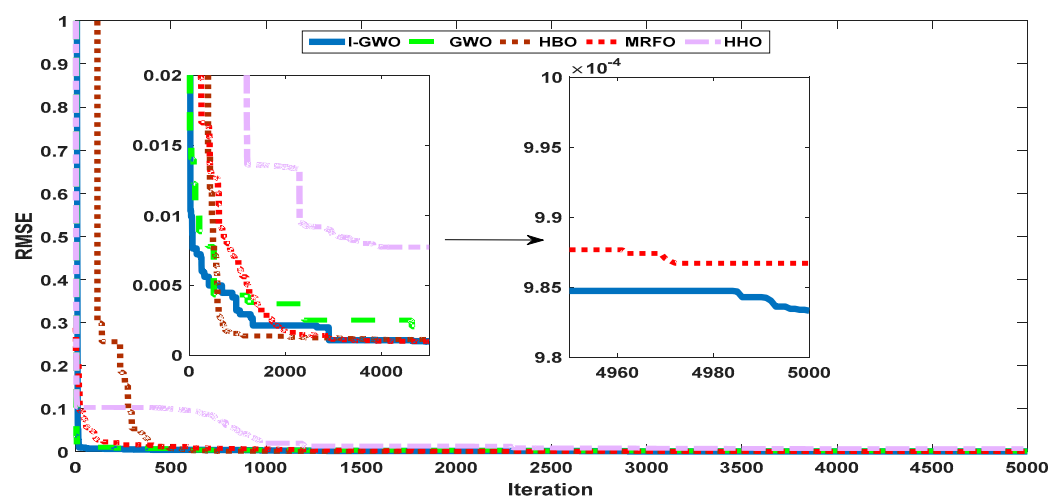


**Figure 4.** The convergence curve of all studied algorithms.

**Table 3.** The statistical results of all algorithms.

	Minimum	Average	Maximum	STD
I-GWO	0.000983	0.000984	0.000985	$6.60404 \times 10^{-7}$
GWO	0.001298	0.00751	0.019319	0.010231343
HBO	0.00112	0.001606667	0.0024	0.000692917
MRFO	0.000986	0.000987	0.000989	$1.25983 \times 10^{-6}$
HHO	0.0077205	0.0117475	0.01917	0.006435824



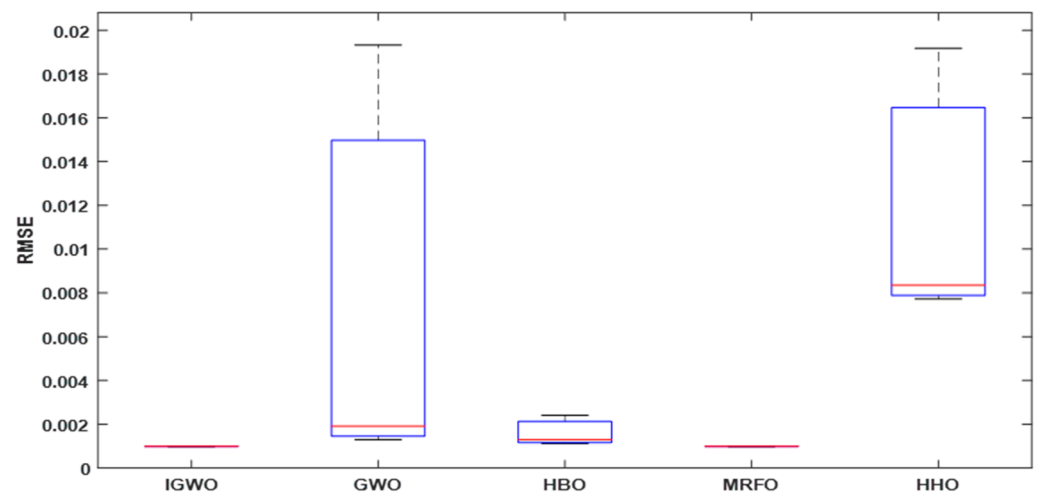


Figure 5. Boxplot of all algorithms for 30 independent runs.

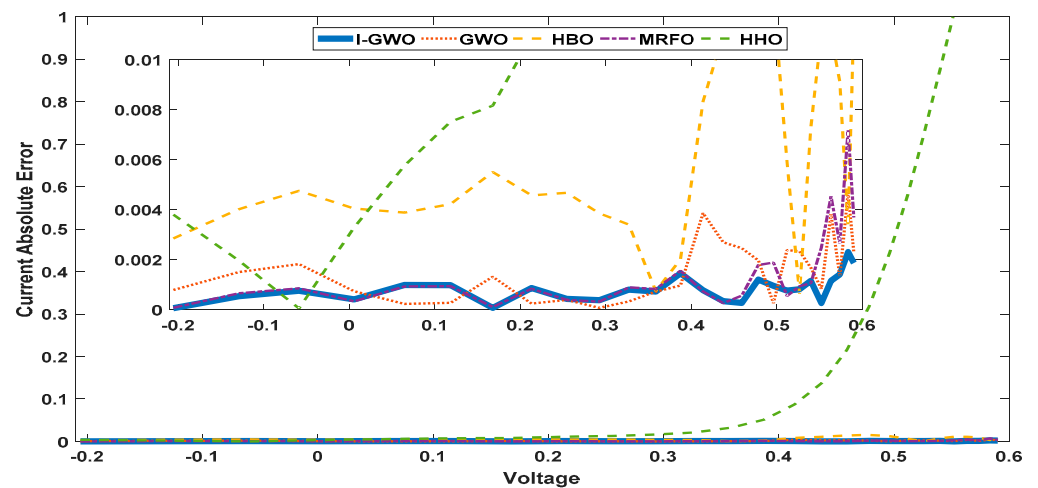


Figure 6. Current absolute error of all studied algorithms.

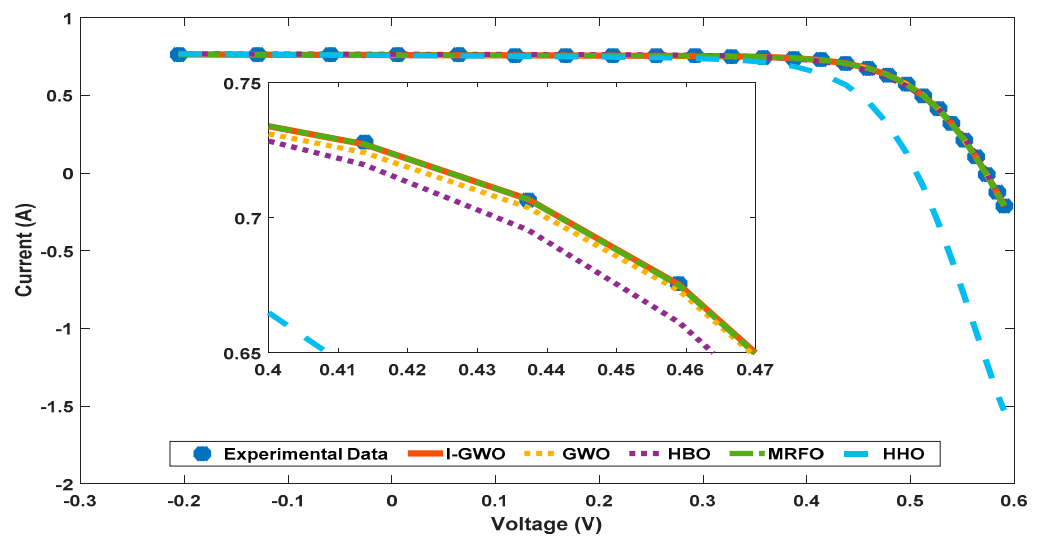


Figure 7. Current-voltage curve for experimental current and TDM current for different algorithms.

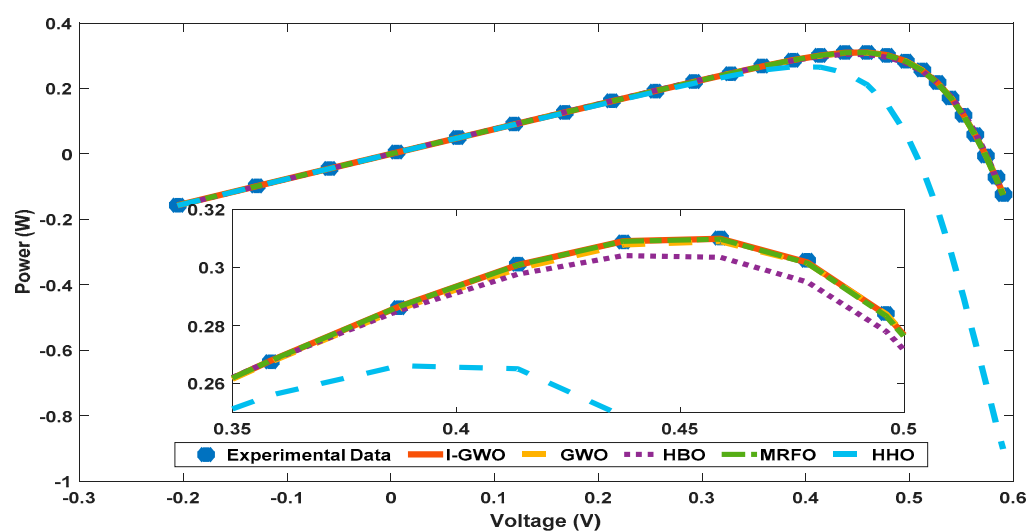


Figure 8. Power-voltage curve for experimental power and TDM power for different algorithms.

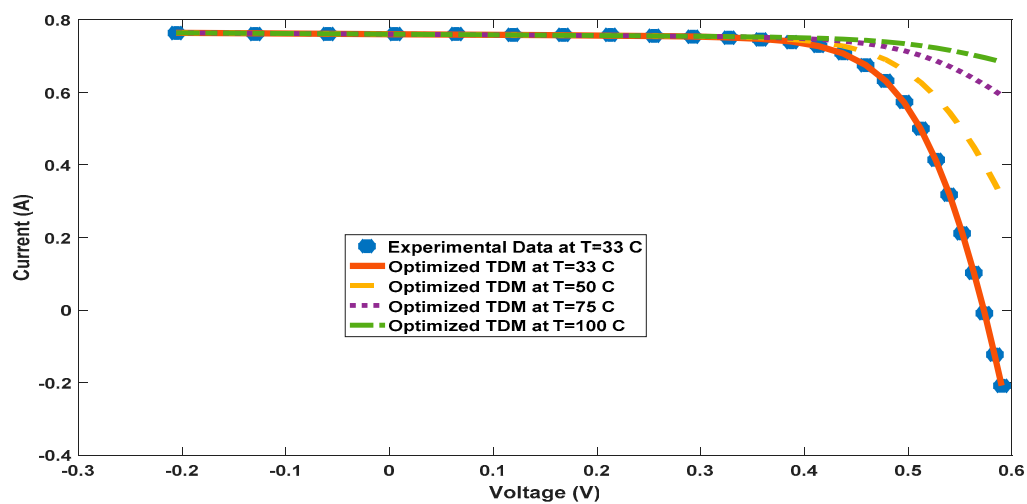


Figure 9. Current-voltage curve for experimental current and TDM current for I-GWO at different temperatures.

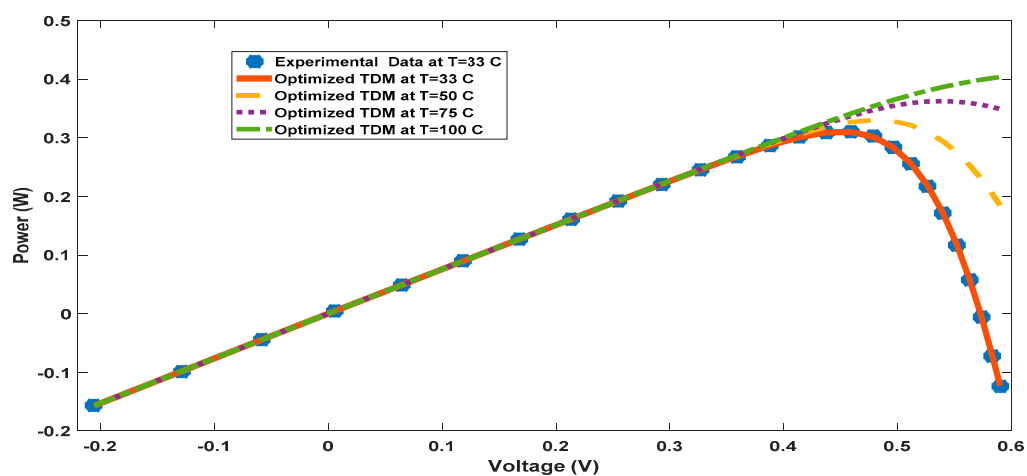
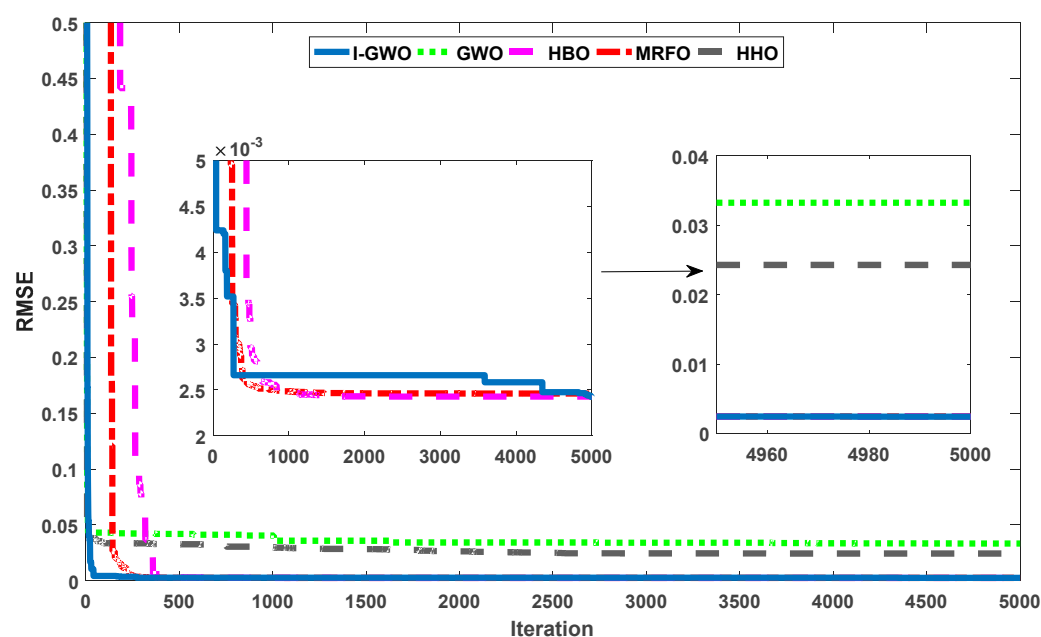
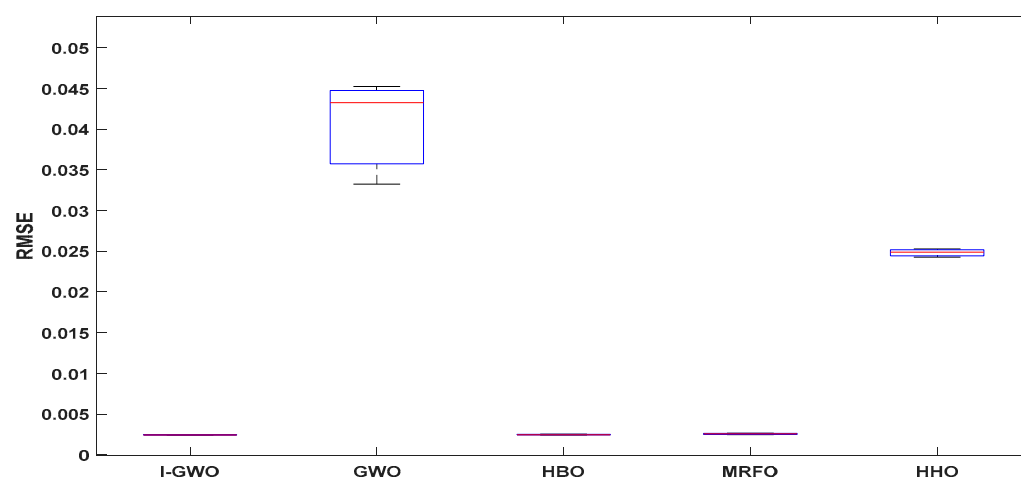


Figure 10. Power-voltage curve for experimental power and TDM power for I-GWO at different temperatures.

**Table 4.** Estimated parameters and RMSE for I-GWO and other optimization algorithms.

	I-GWO	GWO	HBO	MRFO	HHO
Rs( $\Omega$ )	1.198683773	1.666138	1.199582	1.210609373	1.804672596
Rsh( $\Omega$ )	986.3365886	60	983.629	799.9841045	358.9956246
Iph(A)	1.030508846	1.153399	1.030447	1.032037975	1.025407497
Isd1(A)	$1.25 \times 10^{-6}$	$1.48 \times 10^{-10}$	$3.48 \times 10^{-7}$	$6.20 \times 10^{-8}$	$6.07 \times 10^{-10}$
Isd2(A)	$7.77 \times 10^{-7}$	$1.83 \times 10^{-10}$	$1.00 \times 10^{-10}$	$1.97 \times 10^{-6}$	$1.24 \times 10^{-9}$
Isd3(A)	$1.54 \times 10^{-6}$	$2.35 \times 10^{-10}$	$3.19 \times 10^{-6}$	$1.09 \times 10^{-6}$	$4.89 \times 10^{-10}$
N1	49.2667226	28.09997	48.60267	48.2266307	29.89953654
N2	48.38422661	28.13075	49.52947	48.08828143	33.55517196
N3	48.25593375	46.03489	48.56558	48.09442382	29.53540241
RMSE	0.0024276291	0.03323	0.0024281	0.0024609	0.024273

**Figure 11.** The convergence curve of all algorithms.**Figure 12.** Boxplot for all algorithms for 30 independent runs.

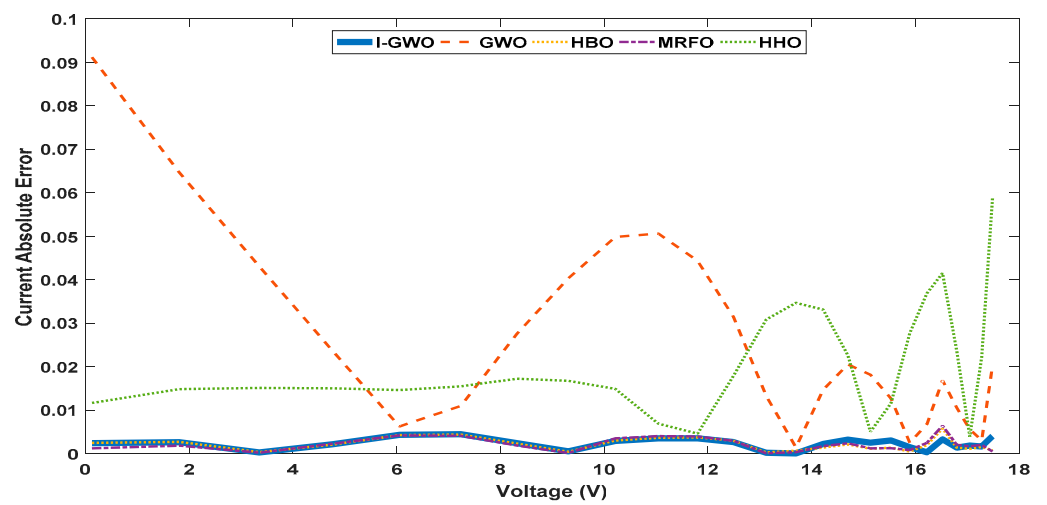


Figure 13. Current absolute error of all algorithms.

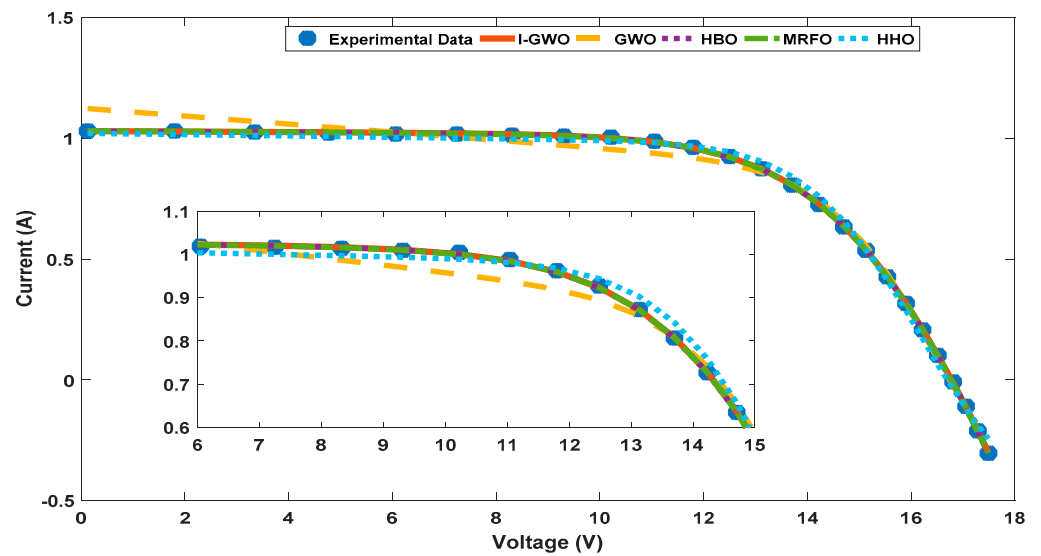


Figure 14. Current-voltage curve for experimental current and TDM current for different algorithms.

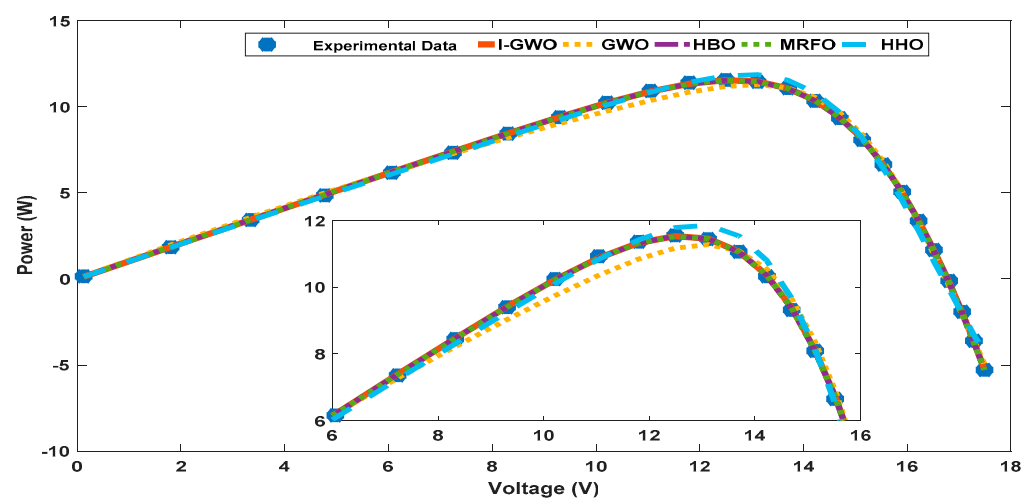
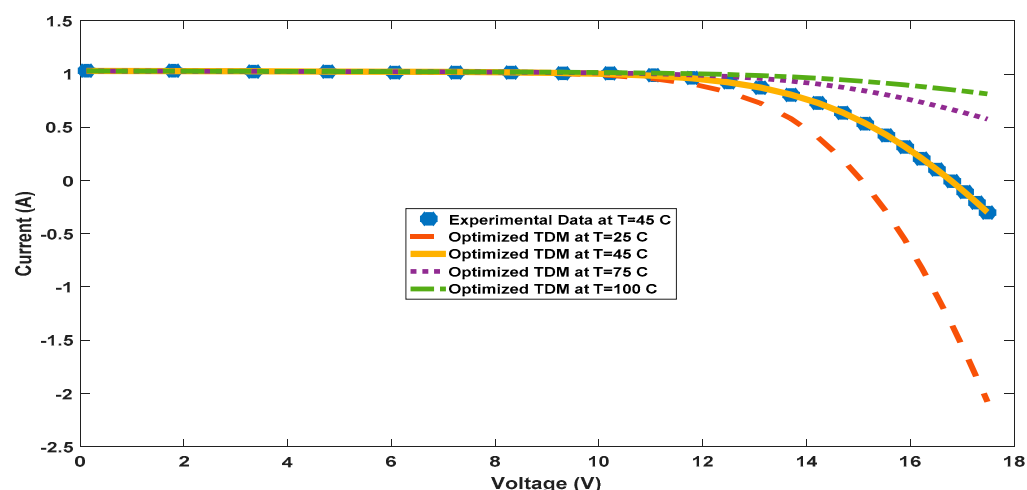
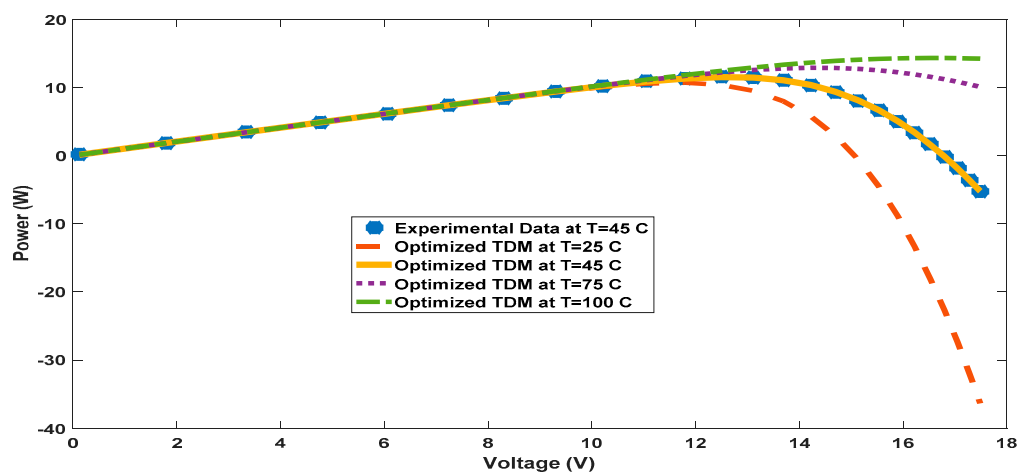


Figure 15. Power-voltage curve for experimental power and TDM power for different algorithms.

**Table 5.** The statistical results of all algorithms.

	Minimum	Average	Maximum	STD
I-GWO	0.002427629	0.002432	0.002438	$5.26003 \times 10^{-6}$
GWO	0.03323	0.040563	0.04523	0.006429101
HBO	0.0024281	0.002465	0.002528	$5.50757 \times 10^{-5}$
MRFO	0.0024609	0.002554	0.002641	$9.0185 \times 10^{-5}$
HHO	0.024273	0.024806	0.025273	0.000503322

**Figure 16.** Current-voltage curve for experimental current and TDM current for I-GWO at different temperatures.**Figure 17.** Power-voltage curve for experimental power and TDM power for I-GWO at different temperatures.

## 5. Overall Discussion

The reliability of I-GWO algorithm has been evaluated by different comparisons with the original GWO and three well known recent algorithms (HBO, MRFO and HHO). I-GWO has been tested for parameters estimation of solar cell and PV panel which considered the most popular real PV system. In the two applications, the I-GWO wins to achieve the best RMSE compared with the four studied algorithms. In Application #1, the RMSE of I-GWO is 0.00098331. This value is better than those obtained by different algorithms proposed in literature such as TLABC, GOTLBO and TLBO [46]. In addition, the accuracy of I-GWO is clear from the current absolute error figure as it has the least error over different measured data. The convergence speed of I-GWO is better than the other algorithms as observed in Figures 4 and 11. The statistical analysis for the results in the two applications prove the

robustness of I-GWO. In Application #1, I-GWO has the lowest minimum and standard deviation values. In Application #2, the minimum value obtained by I-GWO is very close to those obtained by MRFO and HHO and better than others, but it has the lowest standard deviation value. Testing the estimated TDM optimized by I-GWO at different operating temperatures is verified by drawing current–voltage and power–voltage characteristic curves at temperatures for the two applications as shown in Figure 9, Figure 10, Figure 16, Figure 17, respectively.

## 6. Conclusions

This paper discussed the parameters estimation of TDM PV system which is considered one of important topics in the real world due to its cost-impact in PV system manufacturing. This paper proposed an application for I-GWO algorithm to estimate more accurate parameters of PV model. Two real examples were discussed: 57 mm diameter commercial silicon R.T.C France solar cell and polycrystalline PV panel. Many evaluation methods were applied, namely, a comparison of the obtained results between I-GWO and others recent optimization algorithms as well as applying different evaluation factors such as RMSE, absolute error and statistical analysis. The results of the two applied applications are extended to include quantitative and qualitative results. The accuracy of algorithms is compared through RMSE and absolute error as well as statistical analysis to cover different quantitative results. The behavior of algorithms is compared through different qualitative results such as algorithm convergence speed and boxplot graph for all statistical results. This study presented a comparison and discussion of current-voltage characteristics and power-voltage characteristics between real measured data set and PV model optimized by different algorithms. The results show that I-GWO has a significant improvement in accuracy than original GWO and other algorithms and this is made clear by the RMSE for the two applications. This study is considered a starting point for research work that focuses on studying the applicability of this improved algorithm on modeling of complex and large PV systems.

**Author Contributions:** Conceptualization, A.-E.R. and S.K.; methodology, T.K., S.-R.O. and S.-B.R.; software, A.-E.R. and S.K.; validation, T.K., S.-R.O. and S.-B.R.; formal analysis, A.-E.R. and S.K.; investigation, T.K., S.-R.O. and S.-B.R.; resources, A.-E.R. and S.K.; data curation, T.K., S.-R.O. and S.-B.R.; writing—original draft preparation, A.-E.R. and S.K.; writing—review and editing, T.K., S.-R.O. and S.-B.R.; visualization, T.K., S.-R.O. and S.-B.R.; supervision, A.-E.R. and S.K.; project administration, T.K., S.-R.O. and S.-B.R. All authors have read and agreed to the published version of the manuscript.

**Funding:** This work was supported by the “Development of Modular Green Substation and Operation Technology” of the Korea Electric Power Corporation (KEPCO).

**Institutional Review Board Statement:** Not applicable.

**Informed Consent Statement:** Not applicable.

**Data Availability Statement:** Not applicable.

**Conflicts of Interest:** The authors declare no conflict of interest.

## Nomenclature

Symbol	Description
TDM	Three Diode Model
RMSE	Root Mean Square Error
PV	Photo Voltaic
Ns	number of series solar cells
I	PV module output current
NP	number of parallel PV modules
V	Terminal voltage
XP(t)	Prey current position

I <sub>ph</sub>	Photo generated current source
X(t)	Gray wolf current position
$\eta_1$	First Diode Ideality factor (Diffusion current components)
$\eta_2$	Second Diode Ideality Factor (Recombination current components)
$\eta_3$	Third diode Ideality Factor (Leakage current components)
R <sub>sh</sub>	Equivalent Shunt resistance for current leakage resistance across the P-N junction of solar cell
R <sub>s</sub>	Equivalent Series resistance for semiconductor material at neutral regions
K	$=1.380 \times 10^{-23}$ (J/Ko) Boltzmann constant
I <sub>s1</sub>	First diode current
q	$1.602 \times 10^{-19}$ (C) Coulombs.
I <sub>s2</sub>	Second diode current
T (Ko)	Photo cell temperature (Kelvin)
I <sub>s3</sub>	Third diode current
HBO	Heap-based optimizer
X(t)	Current position
X(t + 1)	Position in next iteration
GWO	Grey Wolf Optimizer
I-GWO	Improved Grey Wolf Optimizer
HHO	Harries Hawk optimization
MRFO	Manta Ray Foraging Optimization

## References

- Humada, A.M.; Darweesh, K.G.M.; Kamil, M.; Samen, F.M.; Naseer, K.K.; Tahseen, A.T.; Omar, I.A.; Saad, M. Modeling of PV system and parameter extraction based on experimental data: Review and investigation. *Sol. Energy* **2020**, *199*, 742–760. [\[CrossRef\]](#)
- Gielen, D.; Boshell, F.; Saygin, D.; Bazilian, M.D.; Wagner, N.; Gorini, R. The role of renewable energy in the global energy transformation. *Energy Strategy Rev.* **2019**, *24*, 38–50. [\[CrossRef\]](#)
- Araújo, K.; Boucher, J.L.; Aphale, O. A clean energy assessment of early adopters in electric vehicle and solar photovoltaic technology: Geospatial, political and socio-demographic trends in New York. *J. Clean. Prod.* **2019**, *216*, 99–116. [\[CrossRef\]](#)
- Choudhary, P.; Srivastava, R.K. Sustainability perspectives—A review for solar photovoltaic trends and growth opportunities. *J. Clean. Prod.* **2019**, *227*, 589–612. [\[CrossRef\]](#)
- Singh, S.N.; Prabhakar, T.; Sumit, T. Introduction to solar energy. In *Fundamentals and Innovations in Solar Energy*; Springer: Singapore, 2021; pp. 1–9.
- Piyush, G. Importance of Detailed Modeling of Loads/PV Systems Connected to Secondary of Distribution Transformers. Master's Thesis, Electrical Engineering Faculty of the Virginia Polytechnic Institute and State University, Blacksburg, VA, USA, 2017.
- Halabi, M.A.; Al-Qattana, A.; Al-Otaibi, A. Application of solar energy in the oil industry—Current status and future prospects. *Renew. Sustain. Energy Rev.* **2015**, *43*, 296–314. [\[CrossRef\]](#)
- Mekhilef, S.; Faramarzi, S.Z.; Saidur, R.; Salam, Z. The application of solar technologies for sustainable development of agricultural sector. *Renew. Sustain. Energy Rev.* **2013**, *18*, 583–594. [\[CrossRef\]](#)
- Zhang, Y.; Sivakumar, M.; Yang, S.; Enever, K.; Ramezani-pour, M. Application of solar energy in water treatment processes: A review. *Desalination* **2018**, *428*, 116–145. [\[CrossRef\]](#)
- Sharma, A.; Sharma, A.; Averbukh, M.; Jatelly, V.; Azzopardi, B. An effective method for parameter estimation of a solar cell. *Electronics* **2021**, *10*, 312. [\[CrossRef\]](#)
- Rodrigues, E.M.G.; Melicio, R.; Mendes, V.M.F.; Catalao, J.P. Simulation of a solar cell considering single-diode equivalent circuit model. *RE&PQJ* **2011**. [\[CrossRef\]](#)
- Ma, J.; Man, K.L.; Ting, T.O.; Zhang, N.; Guan, S.U.; Wong, P.W. Wong approximate single-diode photovoltaic model for efficient I-V characteristics estimation. *Sci. World J.* **2013**, *2013*, 230471. [\[CrossRef\]](#) [\[PubMed\]](#)
- Sabadus, A.; Mihailetschi, V.; Paulescu, M. Parameters extraction for the one-diode model of a solar cell. In *AIP Conference Proceedings*; AIP Publishing LLC: Melville, NY, USA, 2017; p. 40005.
- Tamrakar, V.; Gupta, S.C.; Sawle, Y. Single-diode Pv cell modeling and study of characteristics of single and two-diode equivalent circuit. *Electr. Electron. Eng. Int. J.* **2015**, *4*, 12. [\[CrossRef\]](#)
- Tamrakar, V.; Gupta, S.C.; Sawle, Y. Single-diode and two-diode Pv cell modeling using matlab for studying characteristics of solar cell under varying conditions. *Electr. Comput. Eng. Int. J.* **2015**, *4*, 67–77. [\[CrossRef\]](#)
- Sulyok, G.; Summhammer, J. Extraction of a photovoltaic cell's double-diode model parameters from data sheet values. *Energy Sci. Eng.* **2018**, *6*, 424–436. [\[CrossRef\]](#)
- Tanvir, A.; Sobhan, S.; Nayan, M.F. Comparative analysis between single diode and double diode model of PV cell: Concentrate different parameters effect on its efficiency. *J. Power Energy Eng.* **2016**, *4*, 31–46.



18. Soliman, M.A.; Al-Durra, A.; Hasanien, H.M. Electrical parameters identification of three-diode photovoltaic model based on equilibrium optimizer algorithm. *IEEE Access* **2021**, *9*, 41891–41901. [\[CrossRef\]](#)
19. Wang, R. Parameter identification of photovoltaic cell model based on enhanced particle swarm optimization. *Sustainability* **2021**, *13*, 840. [\[CrossRef\]](#)
20. Khanna, V.; Das, B.K.; Bisht, D.; Singh, P.K. A three diode model for industrial solar cells and estimation of solar cell parameters using PSO algorithm. *Renew. Energy* **2015**, *78*, 105–113. [\[CrossRef\]](#)
21. El-Hameed, M.A.; Elkholy, M.M.; El-Fergany, A.A. Three-diode model for characterization of industrial solar generating units using Manta-rays foraging optimizer: Analysis and validations. *Energy Convers. Manag.* **2020**, *219*, 113048. [\[CrossRef\]](#)
22. Harrag, A.; Daili, Y. Three-diode PV model parameters extraction using PSO algorithm. *Rev. Energ. Renouvelables* **2019**, *22*, 85–91.
23. Shekoofa, O.; Wang, J. Multi-diode modeling of multi-junction solar cells In Proceedings of the 23rd Iranian Conference on Electrical Engineering, Tehran, Iran, 10–14 May 2015.
24. Ukoima, K.N.; Ekwe, O. A three-diode model and simulation of photovoltaic (Pv) cells. *J. Eng. Technol.* **2019**, *5*, 108–116.
25. Bayoumi, A.S.; El-Sehiemy, R.A.; Mahmoud, K.; Lehtonen, M.; Darwish, M.M. Assessment of an improved three-diode against modified two-diode patterns of MCS solar cells associated with soft parameter estimation paradigms. *Appl. Sci.* **2021**, *11*, 1055. [\[CrossRef\]](#)
26. Mehdi, O.; Mohamed, S.M.; Djalel, D.O. Comprehensive three-diode model of photovoltaic array with partial shading capability. *Int. J. Power Energy Convers.* **2018**, *9*, 159–173.
27. Saha, C.; Agbu, N.; Jinks, R.; Huda, M.N. Review article of the solar PV parameters estimation using evolutionary algorithms. *MOJ Sol. Photoenergy Syst.* **2018**, *2*, 63–75.
28. Qais, M.H.; Hasanien, H.M.; Alghuwainem, S. Parameters extraction of three-diode photovoltaic model using computation and Harris Hawks optimization. *Energy* **2020**, *195*, 117040. [\[CrossRef\]](#)
29. Abdel-Basset, M.; Mohamed, R.; Mirjalili, S.; Chakraborty, R.K.; Ryan, M.J. Solar photovoltaic parameter estimation using an improved equilibrium optimizer. *Sol. Energy* **2020**, *209*, 694–708. [\[CrossRef\]](#)
30. Sheng, H.; Li, C.; Wang, H.; Yan, Z.; Xiong, Y.; Cao, Z.; Kuang, Q. Parameters extraction of photovoltaic models using an improved moth-flame optimization. *Energies* **2019**, *12*, 3527. [\[CrossRef\]](#)
31. Elazab, O.S.; Hasanien, H.M.; Alsaidan, I.; Abdelaziz, A.Y.; Mueen, S.M. Parameter estimation of three diode photovoltaic model using grasshopper optimization algorithm. *Energies* **2020**, *13*, 497. [\[CrossRef\]](#)
32. Saxena, A.; Sharma, A.; Shekhawat, S. Parameter extraction of solar cell using intelligent grey wolf optimizer. *Evol. Intell.* **2020**. [\[CrossRef\]](#)
33. Nadimi-Shahraki, M.H.; Taghian, S.; Mirjalili, S. An improved grey wolf optimizer for solving engineering problems. *Expert Syst. Appl.* **2021**, *166*, 113917. [\[CrossRef\]](#)
34. Qais, M.H.; Hasanien, H.M.; Alghuwainem, S.; Nouh, A.S. Coyote optimization algorithm for parameters extraction of three-diode photovoltaic model of photovoltaic modules. *Energy* **2019**, *187*, 116001. [\[CrossRef\]](#)
35. Qais, M.H.; Hasanien, H.M.; Alghuwainem, S. Identification of electrical parameters for three-diode photovoltaic model using analytical and sunflower optimization algorithm. *Appl. Energy* **2019**, *250*, 109–117. [\[CrossRef\]](#)
36. Mohamed, A.; Reda, M.; Attia, E.; Mohamed, A.; Askar, S.S. Parameters identification of PV triple-diode model using improved generalized normal distribution algorithm. *Mathematics* **2021**, *9*, 995.
37. Allam, D.; Yousri, D.A.; Eteiba, M.B. Parameters extraction of the three diode model for the multi-crystalline solar cell/module using Moth-Flame Optimization Algorithm. *Energy Convers. Manag.* **2016**, *123*, 535–548. [\[CrossRef\]](#)
38. Mirjalili, S.; Mirjalili, S.M.; Lewis, A. Grey wolf optimizer. *Adv. Eng. Softw.* **2014**, *69*, 46–61. [\[CrossRef\]](#)
39. Roy, R.G.; Ghoshal, D. Grey wolf optimization-based second order sliding mode control for inchworm robot. *Robotica* **2019**, *38*, 1–19. [\[CrossRef\]](#)
40. Luo, K.; Zhao, O. A binary grey wolf optimizer for the multidimensional knapsack problem. *Appl. Soft Comput.* **2019**, *83*, 105645. [\[CrossRef\]](#)
41. Pal, A.; Bahuguna, S. Grey wolf optimizer. *Future Asp. Eng. Sci. Technol.* **2018**, *36*, 379–382.
42. Sharma, I.; Chahar, V.; Agri, S. A comprehensive survey on grey wolf optimization. *Recent Pat. Comput. Sci.* **2020**, *13*, 1–13. [\[CrossRef\]](#)
43. Abdelghany, R.Y.; Kamel, S.; Ramadan, A.; Sultan, H.; Rahmann, C. Solar cell parameter estimation using school-based optimization algorithm. In Proceedings of the IEEE International Conference on Automation/XXIV Congress of the Chilean Association of Automatic Control, Santiago, Chile, 22–26 March 2021.
44. Ramadan, A.; Kamel, S.; Korashy, A.; Yu, J. Photovoltaic cells parameter estimation using an enhanced teaching learning based optimization algorithm. *Iran. J. Sci. Technol.* **2019**, *44*, 767–779. [\[CrossRef\]](#)
45. Ramadan, A.; Kamel, S.; Hussein, N.M.; Hassan, M.H. A new application of chaos game optimization algorithm for parameters extraction of three diode photovoltaic model. *IEEE Access* **2021**, *9*, 51582–51594. [\[CrossRef\]](#)
46. Liao, Z.; Chen, Z.; Li, S. Parameters extraction of photovoltaic models using triple-phase teaching-learning-based optimization. *IEEE Access* **2019**, *7*, 77629–77641. [\[CrossRef\]](#)